FEATURED ARTICLE

PINK1 Heterozygous Mutations Induce Subtle Alterations in Dopamine-Dependent Synaptic Plasticity

Graziella Madeo, MD,[1†] Tommaso Schirinzi, MD,[1†] Giuseppina Martella, PhD,[1] E. Claudio Latagliata, PhD,[2,3] Francesca Puglisi, PhD,[1] Jie Shen, PhD,[4] Enza Maria Valente, MD, PhD,[5,6] Mauro Federici, BSc,[2] Nicola B. Mercuri, MD,[1,2] Stefano Puglisi-Allegra, PhD,[2,3] Paola Bonsi, PhD,[2] and Antonio Pisani, MD, PhD[1,2*]

[1]*Department of System Medicine, University of Rome "Tor Vergata", Rome, Italy*
[2]*Fondazione Santa Lucia, Istituto di Ricovero e Cura a Carattere Scientifico, Rome, Italy*
[3]*Department of Psychology and "Daniel Bovet" Center, Sapienza University of Rome, Rome, Italy*
[4]*Center for Neurologic Diseases, Brigham and Women's Hospital, Program in Neuroscience, Harvard Medical School, Boston, Massachusetts, USA*
[5]*Istituto di Ricovero e Cura a Carattere Scientifico, Casa Sollievo della Sofferenza, Mendel Laboratory, San Giovanni Rotondo, Italy*
[6]*Department of Medicine and Surgery, University of Salerno, Salerno, Italy*

ABSTRACT: Homozygous or compound heterozygous mutations in the phosphatase and tensin homolog-induced putative kinase 1 (*PINK1*) gene are causative of autosomal recessive, early onset Parkinson's disease. Single heterozygous mutations have been detected repeatedly both in a subset of patients and in unaffected individuals, and the significance of these mutations has long been debated. Several neurophysiological studies from non-manifesting *PINK1* heterozygotes have demonstrated the existence of neural plasticity abnormalities, indicating the presence of specific endophenotypic traits in the heterozygous state. We performed a functional analysis of corticostriatal synaptic plasticity in heterozygous PINK1 knockout ($PINK1^{+/-}$) mice using a multidisciplinary approach and observed that, despite normal motor behavior, repetitive activation of cortical inputs to striatal neurons failed to induce long-term potentiation (LTP), whereas long-term depression was normal. Although nigral dopaminergic neurons exhibited normal morphological and electrophysiological properties with normal responses to dopamine receptor activation, a significantly lower dopamine release was measured in the striatum of $PINK1^{+/-}$ mice compared with control mice, suggesting that a decrease in stimulus-evoked dopamine overflow acts as a major determinant for the LTP deficit. Accordingly, pharmacological agents capable of increasing the availability of dopamine in the synaptic cleft restored normal LTP in heterozygous mice. Moreover, monoamine oxidase B inhibitors rescued physiological LTP and normal dopamine release. Our results provide novel evidence for striatal plasticity abnormalities, even in the heterozygous disease state. These alterations might be considered an endophenotype to this monogenic form of Parkinson's disease and a valid tool with which to characterize early disease stage and design possible disease-modifying therapies.

Key Words: PINK1; autosomal recessive Parkinson's disease; heterozygous mutations; synaptic plasticity; striatum

***Correspondence to:** Dr. Antonio Pisani, Department of System Medicine, University of Rome "Tor Vergata," 00133 Rome, Italy; pisani@uniroma2.it

Funding agencies: This study was supported by grants from the Italian Ministry of Health (Giovani Ricercatori 2009), the Italian Ministry of Instruction, University, and Research (MIUR) (PRIN 2011), and the Istituto Nazionale Assicurazione contro Infortuni sul Lavoro (INAIL, project 2/2009) to A.P.; by grants from the Italian Ministry of Health (Ricerca Corrente 2013, Ricerca Finalizzata Malattie Rare 2008, and Giovani Ricercatori 2009), the Italian Telethon Foundation (GGP10140), and MIUR (FIRB Accordi di Programma 2010) to E.M.V.; and by grant NS 041779 from the National Institutes of Health to J.S.

Relevant conflicts of interest/financial disclosures: Nothing to report.
Full financial disclosures and author roles may be found in the online version of this article.

[†]These authors contributed equally to this work.

Received: 23 April 2013; **Revised:** 10 September 2013; **Accepted:** 16 September 2013
Published online 25 October 2013 in Wiley Online Library (wileyonlinelibrary.com). DOI: 10.1002/mds.25724

Gene mutations are causative of distinct inherited forms of Parkinson's disease (PD), playing a relevant role in the etiology of the disease. Mendelian forms of PD account for a relatively small fraction of PD cases, because only 20% of patients who have an early onset and no more than 3% to 5% of those who have a late onset have a monogenic etiology with classical autosomal recessive or dominant inheritance.[1] Homozygous or compound heterozygous mutations in the phosphatase and tensin homolog-induced putative kinase 1 (*PINK1*) gene cause PD with Lewy body pathology, characterized by early onset (often in a limb), slow progression, and a good response to levodopa (L-dopa).[2-4] Single heterozygous mutations or rare variants in the *PINK1* gene have been detected in a subset of patients with sporadic PD (those who have a later onset and clinical features indistinguishable from the features of idiopathic PD) and also in a similar proportion of healthy controls.[3]

Currently, it is believed that the loss of dopaminergic inputs to the dorsal striatum is the major cause for the appearance of motor symptoms in PD,[5,6] which are preceded by a prolonged yet undefined, presymptomatic window characterized by a 30% to 50% reduction in basal ganglia dopamine (DA) levels,[7,8] suggesting a substantial ability to compensate for nigrostriatal cell loss. Functional magnetic resonance imaging studies in clinically unaffected carriers of PINK1 single heterozygous mutations demonstrated an increase in cortical motor-related activity during the execution of self-initiated movements,[9] interpreted as a reorganization of the motor system in the presymptomatic disease stage.[9-11] Moreover, positron emission tomography studies demonstrated a reduced striatal dopaminergic fluorodopa uptake,[11,12] suggesting that the natural progression of subclinical motor signs may precede an overt parkinsonian syndrome. Finally, neurophysiological studies demonstrated impaired temporal discrimination thresholds in PINK1 heterozygous healthy carriers.[13]

Based on such evidence, the condition of a nonmanifesting *PINK1* heterozygous carrier provides a unique model in which to study the effects of subclinical dopaminergic dysfunction on motor learning and plasticity. We performed recordings of slices from heterozygous *PINK1* knockout ($PINK1^{+/-}$)[14] mice and explored how the heterozygous condition may interfere with the normal expression of synaptic plasticity at corticostriatal synapses and with nigral dopaminergic neuron excitability. In addition, this electrophysiological study was paralleled by behavioral and neurochemical analyses.

Materials and Methods

PINK1 Mice and Genotyping

Animal experiments were carried out in accordance with the European Commission, Internal Institutional Review Committee, European Union directives, and Italian rules (86/609/EEC, D.Lvo 116/1992, 63/2100 EU, 153/2001A-IHM, and 5/2010 UV). Mice were generated and characterized as reported previously.[14] Breeding colonies of homozygous ($PINK^{-/-}$) mice, heterozygous knockout ($PINK1^{+/-}$) mice, and their wild-type littermates ($PINK1^{+/+}$) were established at our animal house. All experiments were performed blindly. For genotyping, DNA was isolated from mouse tail using the Extract-N-Amp Tissue polymerase chain reaction (PCR) kit (XNAT2; Sigma-Aldrich, Milan, Italy). To amplify the 324-base pair (bp) and 501-bp fragments, three specific primers were used (10 μM: PINK1-F, 5′ AGA GGA TGC TAG TCC CTG TGA AGG G 3′; PINK1-X, 5′ ACA CTC AGT CCT TGG GCA ATG CTA 3′; NeoA, 5′ ACC AAA GAA GGG AGC CGG TTG 3′). PCR reactions were carried out using the Extract-N-Amp PCR reaction mix (XNAT2 kit) in a My Cycler thermal cycler (Bio-Rad Laboratories, Milan, Italy) for 35 cycles at an annealing temperature of 62°C. The 324-bp and 501-bp sequences were identified with 1.5% agarose gel electrophoresis using 2% SYBR Safe (Bio-Rad Laboratories). Representative images of PCR products separated onto 1.5% agarose gels (Fig. 1A) show the differences between genotypes. In Figure 1A, lane 2 identifies heterozygous mice.

Tissue Slice Preparation

All efforts were made to minimize the number of animals used and to reduce their suffering. The mice were killed, and corticostriatal parasagittal and nigral horizontal slices (290–350 μm) from the substantia nigra pars compacta (SNpc) were prepared as described previously[15-18] in Krebs' solution bubbled with 95% O_2 and 5% CO_2. Individual slices were transferred into a recording chamber superfused with oxygenated Krebs' medium and were maintained at 32°C to 33°C. Nigral slices were kept at 34°C to 35°C.

Electrophysiology

Whole-cell patch-clamp recordings were obtained from medium spiny neurons (MSNs), which were visualized using infrared videomicroscopy, as described previously.[14,18] The recordings were made with an AxoPatch 200B amplifier coupled to *pClamp 10.2* software (Molecular Devices LLC, Sunnyvale, CA, USA) using borosilicate glass pipettes (resistance, 2.5-5 MΩ). Membrane currents were continuously monitored, and access resistance (measured using voltage-clamp analysis) was in the range from 5 to 30 MΩ before electronic compensation (routinely, this is 60%-80%). Cells that showed a change $\geq$ 20% in series resistance during the experiment were discarded from the analysis. An internal solution with the following composition was used: 120 mM Cs-gluconate;

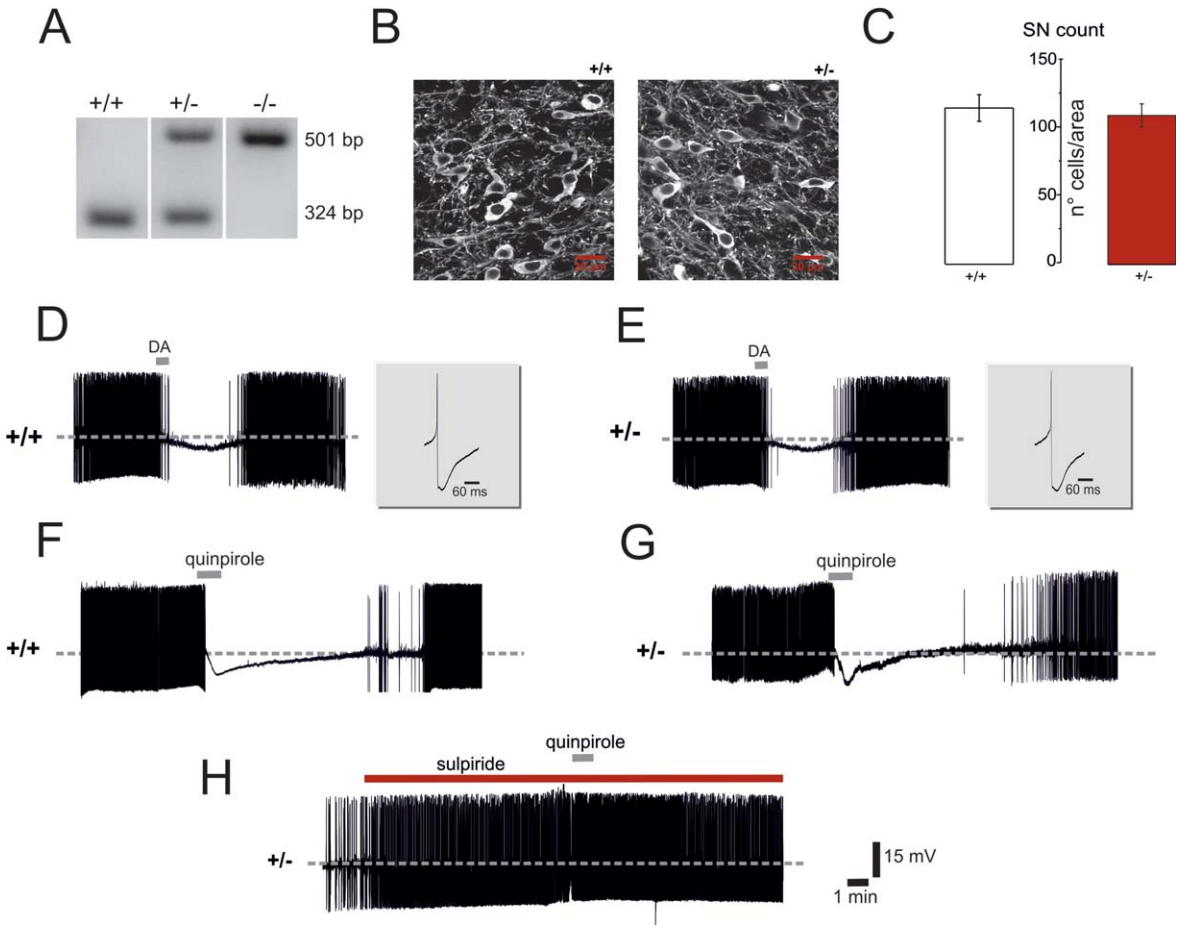

FIG. 1. These images characterize mouse genotypes and dopaminergic nigral cells. (**A**) Wild-type phosphatase and tensin homolog-induced putative kinase 1 (*PINK1*) (PINK1$^{+/+}$), heterozygous *PINK1* knockout (PINK1$^{+/-}$), and homozygous (PINK1$^{-/-}$) mouse genotypes were analyzed. Representative gel images of polymerase chain reaction products are shown. Products from PINK1$^{+/+}$, PINK1$^{+/-}$, and PINK1$^{-/-}$ mice appear in lanes 1, 2, and 3, respectively (lane 1, a 324-base pair [bp] fragment; lane 3, a 501-bp fragment; lane 2, both fragments). (**B**) Representative confocal microscope images (z-series projections) show tyrosine hydroxylase (TH) immunostaining in substantia nigra pars compacta (SN) slices. Similar TH immunoreactivity was observed in PINK1$^{+/-}$ mice compared with their PINK1$^{+/+}$ littermates. (**C**) The plot shows similar TH-positive cell counts in the two genotypes in a total area of 425 × 425 μm analyzed for each SN slice. Scale bar = 20 μm. (**D,E**) Sharp microelectrode recordings of dopaminergic neurons from nigral slices obtained from PINK1$^{+/+}$ and PINK1$^{+/-}$ mice, respectively, illustrate typical, spontaneous, rhythmic firing activity. In slices from both genotypes, brief dopamine (DA) application (100 μM, 30 seconds) hyperpolarizes the cell membrane and blocks the firing activity. Upon DA washout, the membrane slowly recovers, and action potential discharge returns to control levels. The *insets* show normal amplitude and duration of single action potentials recorded from dopaminergic neurons in the two genotypes. (**F,G**) Representative traces show the effects of the D2R agonist quinpirole (300 nM, 1 minute) on nigral dopaminergic neurons. Bath-applied quinpirole hyperpolarizes the cell membrane and abolishes the spontaneous firing activity of neurons recorded from PINK1$^{+/+}$ and PINK1$^{+/-}$ mice, respectively. Similar responses are recorded from the two groups of mice. Upon quinpirole washout, the membrane slowly returns to the pre-drug level, and firing activity resumes. (**H**) The quinpirole effect is prevented by pretreatment of the slice with the D2R antagonist sulpiride (3 μM), confirming the specificity of the response. [Color figure can be viewed in the online issue, which is available at wileyonlinelibrary.com.]

13.6 mM CsCl; 10 mM 2-(4-[2-hydroxyethyl]piperazine-1-yl)ethanesulfonic acid (HEPES); 1.1 mM ethylene glycol tetraacetic acid (EGTA); 0.1 mM $CaCl_2$; 2.5 mM Mg-adenosine triphosphate (ATP); and 0.3 mM Na-guanosine triphosphate (GTP), pH 7.3.[19,20]

For spontaneous glutamatergic excitatory postsynaptic currents (sEPSCs), MSNs were clamped at a holding potential of − 60 mV[20] in the presence of picrotoxin (50 μM). sEPSCs were completely blocked by the N-methyl-D-aspartate (NMDA) and α-amino-3-hydroxy-5-methyl-4-isoxazolepropionic acid (AMPA) receptor antagonists MK-801 (30 μM) and CNQX (10 μM), respectively. Conversely, spontaneous γ-aminobutyric acid (GABA)ergic inhibitory postsynaptic currents (sIPSCs) were recorded at a holding potential of + 10 mV in the presence of MK-801 and CNQX. In these conditions, sIPSCs were blocked by picrotoxin. To isolate both miniature EPSCs (mEPSCs) and miniature inhibitory postsynaptic currents (mIPSCs) tetrodotoxin (TTX) (1 μM), was added to the perfusing solution.

Sharp-Electrode Recordings of Striatal and Nigral Neurons

Intracellular recording electrodes were filled with 2 M KCl (30–60 MΩ). Signals were recorded with an Axoclamp 2B amplifier, displayed on an oscilloscope,

and stored on a computer using a Digidata 1322A device and *pClamp 10.2* software (Crisel Instr., Rome, Italy). A bipolar electrode was used to evoke corticostriatal excitatory postsynaptic potentials (EPSPs). Test stimuli were delivered at 0.1 Hz in picrotoxin. This electrophysiological approach was used to retain the fidelity of postreceptor signaling in synaptic plasticity experiments. For the high-frequency stimulation (HFS) protocol (three trains: 3-second duration, 100-Hz frequency, 20-second intervals), stimulus intensity was raised to suprathreshold levels. The amplitude of EPSPs was averaged and plotted as a percentage of the control amplitude for 15 minutes before protocol induction. To optimize long-term potentiation (LTP) induction, magnesium was omitted from the external medium.[17] Nigral recordings were performed as described previously.[15,21-24] Dopaminergic neurons from the SNpc were identified by their electrophysiological properties. Traces were stored in *pClamp 10.2* running on a computer for off-line analysis.

Drug Source and Statistical Analysis

Drugs were obtained from Tocris Cookson Ltd. (Bristol, UK), except for dopamine, nomifensine, L-dopa, and tyramine (Sigma-Aldrich). Amphetamine was provided by Dr. N.B. Mercuri. Patch-clamp data were analyzed offline using *Clampfit 10.2* (Crisel Instr., Rome, Italy), *Origin 8* (Originlab Corporation, Northampton, MA, USA), and *Mini-Analysis 6.0* (Synaptosoft, Decatur, GA, USA) software. For analyzing spontaneous and miniature postsynaptic currents, the detection threshold (3–5 pA) was set to twice the noise after trace filtering (traces in the figures are not filtered). For data presented as mean ± standard error of the mean, statistical significance between groups was evaluated using a paired Student *t* test, an unpaired Student *t* test, or the Wilcoxon rank-sum test. Percentage values were calculated for each individual experiment, and all data are presented as the mean ± standard error of the mean for each condition. The Student *t* test and the non-parametric Mann-Whitney test were used to compare means before HFS and after HFS/drug. An analysis of variance with the Tukey's post-hoc test was performed among groups ($P < 0.05$; $\alpha = 0.01$). *P* values < 0.05 were considered statistically significant.

Voltammetry

Amperometric detection of DA was obtained as described previously.[23] The tips of the carbon fiber electrodes (World Precision Instruments GmbH, Berlin, Germany) were gently positioned into corticostriatal slices. Constant potential amperometry was obtained with a World Precision Instruments MicroC holding the electrodes at an oxidation potential of 0.55 to 0.60 V versus reference electrode Ag/AgCl.[25,26] Currents sampled at this oxidation peak potential were measured to provide profiles of DA concentration ([DA]o) versus time. Electrode calibration was obtained by bath-perfusing DA (0.3–10 μM) in all experimental media. A supramaximal electrical stimulation of the striatum was obtained with a pulse of 1 mA for 80 μsec. Data were analyzed using a Student *t* test.

Histology and Immunohistochemistry

Histological samples were obtained from perfused animals and biocytin-loaded slices from both genotypes. Immediately after recording, the slices that contained biocytin-loaded cells were fixed in 4% paraformaldehyde in 0.1 M phosphate buffer (PB) overnight at 4°C. The slices were subsequently immersed in 30% PB/sucrose at 4°C and were then frozen with dry ice and cut into 35-μm-thick transverse sections. The sections derived from biocytin-loaded slices were incubated with cyanine dye 2 (Cy2)-conjugated or Cy3-conjugated streptavidin (1:200 dilution; Jackson ImmunoResearch Laboratories, Inc., West Grove, PA, USA) in PB/0.3% Triton X-100 for 1 hour at room temperature, and images were acquired as previously described.[17]

For an immunostaining assay, mice were deeply anesthetized (tribromoethanol, 0.002 mL/0.01 kg) and perfused with ice-cold 4% paraformaldehyde. The dissected brains were equilibrated with 30% sucrose overnight for three nights, and 30-μm-thick coronal sections were cut. Slices were preincubated with 10% normal donkey serum solution (NDS) in phosphate-buffered saline (PBS)/0.25% Triton X-100 (TPBS) for 1 hour at room temperature and were incubated with the primary antibody (rabbit polyclonal anti-tyrosine hydroxylase; 1:1,500 dilution; cod. ab112; Abcam, Cambridge, UK) at + 4°C overnight in TPBS/1% NDS. After 3 washes (10 minutes each) with TPBS, the sections were incubated with Cy3-conjugated donkey anti-rabbit secondary antibody (cod. 711-165-152; Jackson ImmunoResearch Laboratories, Inc.) in a 1:200 dilution for 2 hours at room temperature. The sections were washed three times (the last wash was in 4′,6-diamidino-2-phenylindole [DAPI], 0.01 mg/mL), mounted with Vectashield (Vector Laboratories Ltd., Peterborough, UK) on plus-polarized glass slides, and coverslipped. To test for the specificity of the antisera, primary antibody was substituted with normal serum and, accordingly, the immunolabeling was absent (data not shown). Images were acquired with a Zeiss LSM 700 confocal laser scanning microscope (Carl Zeiss AG, Oberkochen, Germany) as previously described.[27] For quantitative analysis, an area of 425 × 425 μm corresponding to the SNpc was selected to manually count the tyrosine hydroxylase (TH)-positive cells in serial coronal sections from adult PINK1$^{+/-}$ mice and PINK1$^{+/+}$ mice.

Behavior

Locomotor activity was assessed in PINK1$^{+/+}$ mice (n = 6) and PINK1$^{+/-}$ mice (n = 6). The apparatus

comprised five gray, opaque Plexiglas chambers (20 × 10 cm) placed inside a sound-attenuated room. Individual mice were introduced into each chamber and accustomed to the apparatus for 60 minutes. Then, all mice were removed and left undisturbed inside their home cages.[28] Subsequently, the mice were placed individually in the same cages they had experienced and were tested for 60 minutes. Behavioral data were collected and analyzed using the EthoVision fully automated video tracking system (Noldus Information Technology BV, Wageningen, the Netherlands).[29] Briefly, a charge coupled device video camera was used to record the experimental system. The signal was then digitized (using a hardware device called a frame grabber) and passed to the computer's memory. Then, digital data were analyzed using *EthoVision* software to measure the "distance moved" (in cm) as an estimate of locomotor activity.

Rotarod

Motor coordination and balance were assessed (n = 5 per genotype) using the Accelerating Rotarod apparatus (model 7650; UGO Basile, Comerio, Italy). The test phase consisted of three trials, of a maximum 300 seconds, separated by 15-minute inter-trial intervals.[30] The rod was initially rotating at a constant speed of 4 revolutions per minute (rpm) to allow positioning of all mice in their respective lanes. Once all mice were positioned, the trial was started, and the rod accelerated from 4 rpm to 40 rpm in 5 minutes. The latency at which each mouse fell off the rod was measured. Data were analyzed using a two-tailed nonparametric Mann-Whitney test.

Results

Cell Count and Activity of Nigral Dopaminergic Neurons Are Unaffected in Heterozygous PINK1 Mice

Neurodegeneration of nigral neurons is a pathological hallmark of PD. However, in prodromal and early disease stages, no obvious depletion has been reported.[31-34] Previous evidence revealed the absence of significant neuronal loss in the SNpc of PINK1$^{-/-}$ mice at ages 2 to 3 months and 8 to 9 months.[14] Similarly, our morphological characterization of the SNpc in PINK1$^{+/-}$ mice did not reveal significant alterations of nigral dopaminergic neurons compared with controls. We performed immunofluorescence experiments with specific antibodies for TH to detect nigral dopaminergic neurons. In serial coronal sections of both PINK1$^{+/-}$ mice and PINK1$^{+/+}$ mice, no macroscopic alterations in the morphology or density of dopaminergic cell bodies or terminals were detected (data not shown). TH-immunoreactive neurons counted in the SNpc did not differ significantly in the number of nigral dopaminergic neurons between PINK1$^{+/-}$ mice and PINK$^{+/+}$ mice ($P > 0.05$; PINK1$^{+/+}$, 115 ± 4.9 neurons; PINK1$^{+/-}$, 114.8 ± 2.9 neurons) (Fig. 1B,C).

Recordings of nigral neurons indicated no significant change in the firing activity from PINK1$^{+/-}$ mice or PINK1$^{+/+}$ mice (PINK1$^{+/+}$, 3.6 ± 1.6 Hz [n = 17]; PINK1$^{+/-}$, 3.52 ± 1.9 Hz [n = 14]; $P > 0.05$; Mann-Whitney test) (Fig. 1D,E). In slices from PINK1$^{+/+}$ mice and PINK1$^{+/-}$ mice, bath application of DA (100 μM for 30 seconds) inhibited cell firing and hyperpolarized the cell membrane (PINK1$^{+/+}$, 5.4 ± 1.3 mV; PINK1$^{+/-}$, 4.9 ± 2 mV; n = 9 per group) (Fig. 1D,E). Upon washout, resting membrane potential gradually recovered, and action potential discharge returned to control levels (Fig. 1D,E). The inhibitory effect of DA on nigral neurons is mediated specifically by somatodendritic D2 autoreceptors (D2R), because it is completely blocked by D2R antagonists[34] and is absent in D2R knockout mice.[15] Accordingly, the D2R agonist quinpirole (300 nM for 1 minute) caused longer lasting membrane hyperpolarization and blockade of the firing discharge in dopaminergic neurons from PINK1$^{+/+}$ mice versus PINK1$^{+/-}$ mice (8.82 ± 3.3 minutes vs. 8.82 ± 2.9 minutes [n = 8 per genotype]; $P > 0.05$) (Fig. 1F,G), an effect that was prevented by application of the D2R antagonist sulpiride (3 μM) (Fig. 1H).

Behavioral Analysis

We assessed the locomotor activity of PINK1$^{+/-}$ mice using a battery of behavioral tests. First, we analyzed spontaneous locomotor activity and observed no statistical difference between the two genotypes in the total distance travelled (Fig. 2A,B) (session 1: PINK1$^{+/+}$, 7,833.8 ± 589.8 cm; PINK1$^{+/-}$, 7,457.9 ± 610.9 cm [n = 6 per genotype]; $P > 0.05$; two-tailed Mann-Whitney test; session 2: PINK1$^{+/+}$, 5,897.6 ± 457.7 cm; PINK1$^{+/-}$, 6,015.7 ± 568.4 cm [n = 6 per genotype]; $P > 0.05$; two-tailed Mann-Whitney test). Next, motor ability was further assessed by means of an accelerated rotarod test. It is noteworthy that PINK1$^{+/-}$ mice performed the same as their respective controls (Fig. 2C) (mean latency to fall: PINK1$^{+/+}$, 270 ± 12.4 seconds; PINK1$^{+/-}$, 284.9 ± 15.1 seconds [n = 5 per genotype]; $P > 0.05$; two-tailed Mann-Whitney test).

Electrophysiological Properties of Striatal Medium Spiny Neurons Are Not Altered in Heterozygous PINK1 Mice

Several genetic mouse models of PD exhibit the dysregulation of striatal circuitry.[14,35,36] We obtained recordings of striatal MSNs from PINK1$^{+/-}$ and PINK1$^{+/+}$ slices. MSNs had similar resting membrane potential (PINK1$^{+/+}$, − 82 ± 3.15 mV [n = 28]; PINK1$^{+/-}$, − 83.4 ± 3.9 mV [n = 32]; $P > 0.05$; Mann-

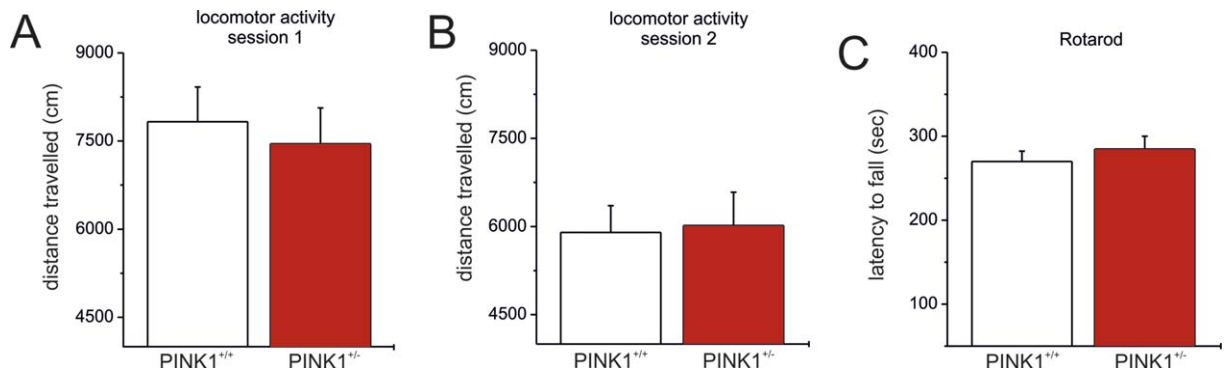

FIG. 2. Normal behavioral ability is illustrated in heterozygous phosphatase and tensin homolog-induced putative kinase 1 (*PINK1*) knockout (PINK1$^{+/-}$) mice. (**A,B**) Spontaneous locomotor activity of PINK1$^{+/-}$ mice did not differ from that of their respective controls (wild-type [PINK1$^{+/+}$] mice). There were no significant differences between the two genotypes in the total distance traveled in either experimental session. (**C**) PINK1$^{+/-}$ mice also demonstrated normal motor coordination and balance on the accelerated rotarod test. Each value is expressed as the mean ± standard error of the mean. [Color figure can be viewed in the online issue, which is available at wileyonlinelibrary.com.]

Whitney test) and were silent at rest; and current pulses caused tonic action potential discharge and strong inward rectification that did not differ among genotypes (Fig. 3A). In an analysis of short-term synaptic plasticity, EPSPs and the paired-pulse ratio were unchanged in PINK1$^{+/-}$ MSNs (data not shown; $P > 0.05$). Random labeling with biocytin confirmed the peculiar features of MSNs, with medium-sized somata (10–20 μm) and extensive, spiny dendritic trees (Fig. 3B). To detect possible changes in the probability of glutamate release, sEPSCs were recorded in the presence of the $GABA_A$ receptor antagonist picrotoxin (50 μM). The frequency and amplitude of glutamate-dependent sEPSCs did not differ between PINK1$^{+/+}$ MSNs (n = 12) and PINK1$^{+/-}$ MSNs (n = 14) (Fig. 3C) (frequency: PINK1$^{+/+}$, 5.34 ± 0.1 Hz; PINK1$^{+/-}$, 4.63 ± 0.2 Hz; amplitude: PINK1$^{+/+}$, 9.44 ± 0.6 pA; PINK1$^{+/-}$, 9.62 ± 0.6 pA; $P > 0.05$; *t* test). Kinetic properties, such as rise time, decay time constant, and half width, were similar (results not shown; $P > 0.05$). Next, we recorded mEPSCs in the presence of TTX to block action potential-dependent glutamate release. As expected, TTX homogenously reduced mean frequencies, but not the mean amplitude, of spontaneous events in both PINK1$^{+/+}$ MSNs (n = 10) and PINK1$^{+/-}$ MSNs (n = 8) (Fig. 3C) (frequency: PINK1$^{+/+}$, 3.41 ± 0.57 Hz; PINK1$^{+/-}$, 2.99 ± 0.14 Hz; amplitude: PINK1$^{+/+}$, 9.32 ± 0.7 pA; PINK1$^{+/-}$, 9.25 ± 0.81 pA; $P > 0.05$; *t* test). Likewise, the mean amplitude and frequencies of GABAergic sIPSCs were comparable between genotypes (Fig. 3D) (frequency: PINK1$^{+/+}$, 2.24 ± 0.27 Hz; PINK1$^{+/-}$, 1.46 ± 0.3 Hz; amplitude: PINK1$^{+/+}$, 15.26 ± 0.42 pA; PINK1$^{+/-}$, 14.98 ± 0.8 pA [n = 9 for each genotype]; $P > 0.05$; Wilcoxon test). Bath application of TTX resulted in a reduction in mean frequencies, but not in the mean amplitude, of mIPSCs in both PINK1$^{+/+}$ MSNs and PINK1$^{+/-}$ MSNs (Fig. 3D) (frequency: PINK1$^{+/+}$, 1.49 ± 0.2 Hz; PINK1$^{+/-}$, 0.62 ± 0.11 Hz; amplitude: PINK1$^{+/+}$, 15.32 ± 0.56 pA; PINK1$^{+/-}$, 15.09 ± 0.6 pA [n = 11 for each genotype]; $P > 0.05$ Wilcoxon). Kinetic properties were unaltered (results not shown).

Selective Dopamine-Dependent Long-term Potentiation Deficit in Heterozygous *PINK1* Mice

We previously demonstrated that PINK1 inactivation is responsible for a marked impairment of bidirectional striatal synaptic plasticity.[14] Therefore, in an attempt to better characterize whether the heterozygous *PINK1* gene mutation may influence corticostriatal synaptic plasticity, we analyzed long-term depression (LTD) and LTP. HFS of glutamatergic afferents in the presence of picrotoxin led to the induction of a robust LTD in MSNs in parasagittal slices from PINK1$^{+/+}$ mice (54.62% ± 4.48% of controls; measured 25 minutes after HFS; n = 25) (Fig. 4A). Similarly, in MSNs from PINK1$^{+/-}$ mice, HFS was able to cause an LTD that was indistinguishable from the LTD measured in wild-type mice (Fig. 4A) (57.43% ± 5.13% of controls; measured 25 minutes after HFS; n = 28; $P > 0.05$; analysis of variance).

Removal of magnesium from the perfusing solution reportedly reveals an NMDA-mediated component of EPSPs and optimizes LTP induction.[37] Accordingly, our HFS protocol invariably induced LTP in PINK1$^{+/+}$ MSNs (Fig. 4B) (172.48% ± 4.45 % of controls; measured 25 minutes after HFS; n = 23; $P < 0.05$; Mann-Whitney test). Unexpectedly, LTP amplitude in PINK1$^{+/-}$ MSNs was significantly lower (137.7% ± 6.4 %; measured 25 minutes after HFS; n = 32; $P < 0.05$; *t* test) (Fig. 4B). The impairment of bidirectional plasticity also could be observed in PINK1$^{-/-}$ mice, as previously reported (data not shown).

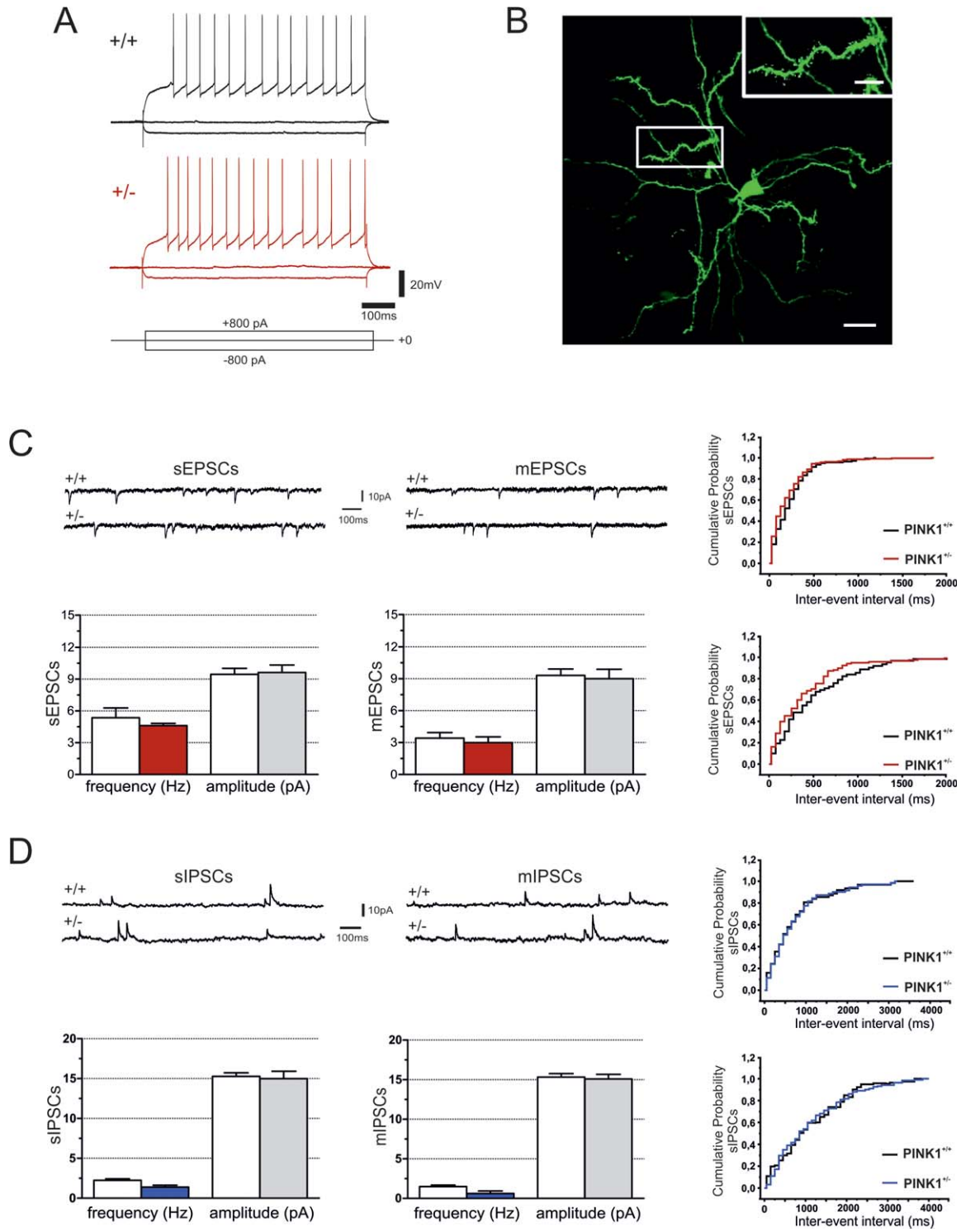

FIG. 3. Normal intrinsic electrophysiological properties of striatal medium spiny neurons (MSNs) are illustrated in heterozygous phosphatase and tensin homolog-induced putative kinase 1 (*PINK1*) knockout *(*PINK1$^{+/-}$) mice. (**A**) Representative traces of current-clamp sharp microelectrode recordings obtained from both wild-type (PINK1$^{+/+}$) medium spiny neurons (MSNs) and PINK1$^{+/-}$ MSNs illustrate tonic firing activity induced by a depolarizing current step (800 pA, 700 msec). The long, depolarizing ramp to spike threshold and the strong, inward rectification during hyperpolarizing steps are peculiar features of MSNs. Note that similar voltage responses are observed in MSNs from both PINK1$^{+/+}$ mice and PINK1$^{+/-}$ mice. (**B**) This confocal microscope image of a biocytin-loaded MSN was recorded from a PINK1$^{+/-}$ slice. Note the branched dendrites densely embedded with spines. Scale bars = 20 μm. (**C**) Whole-cell recordings of spontaneous glutamatergic excitatory postsynaptic currents (sEPSCs) and miniature glutamatergic excitatory postsynaptic currents (mEPSCs) (downward deflections) were recorded from MSNs in the presence of either picrotoxin (50 μM) or picrotoxin plus tetrodotoxin (TTX) (1 μM), respectively, in PINK1$^{+/+}$ and PINK1$^{+/-}$ mice (holding potential, − 60 mV). The plots show no significant changes in mean frequency or amplitude in PINK1$^{+/-}$ mice compared with their wild-type littermates in sample neurons. This representative cumulative probability plot of inter-event intervals confirms that there was no significant change in the frequency of glutamate-mediated events in the two strains. (**D**) Sample traces of spontaneous γ-aminobutyric acid (GABA)ergic inhibitory postsynaptic currents (sIPSCs) and miniature GABAergic inhibitory postsynaptic currents (IPSCs) (upward deflections) were recorded from MSNs in the presence of the N-methyl-D-aspartate (NMDA) receptor antagonist MK-801 (30 μM) and the α-amino-3-hydroxy-5-methyl-4-isoxazolepropionic acid (AMPA) receptor antagonist CNQX (10 μM) in slices from both genotypes (holding potential, + 10 mV). mIPSCs were recorded in TTX. The graphs indicate no significant difference in mean frequency or amplitude among PINK1$^{+/-}$ mice compared with PINK1$^{+/+}$ mice. The representative cumulative probability plot of inter-event intervals reveals no significant difference in the frequency of GABA-dependent currents in sample neurons. Each value is expressed as the mean ± standard error of the mean. [Color figure can be viewed in the online issue, which is available at wileyonlinelibrary.com.]

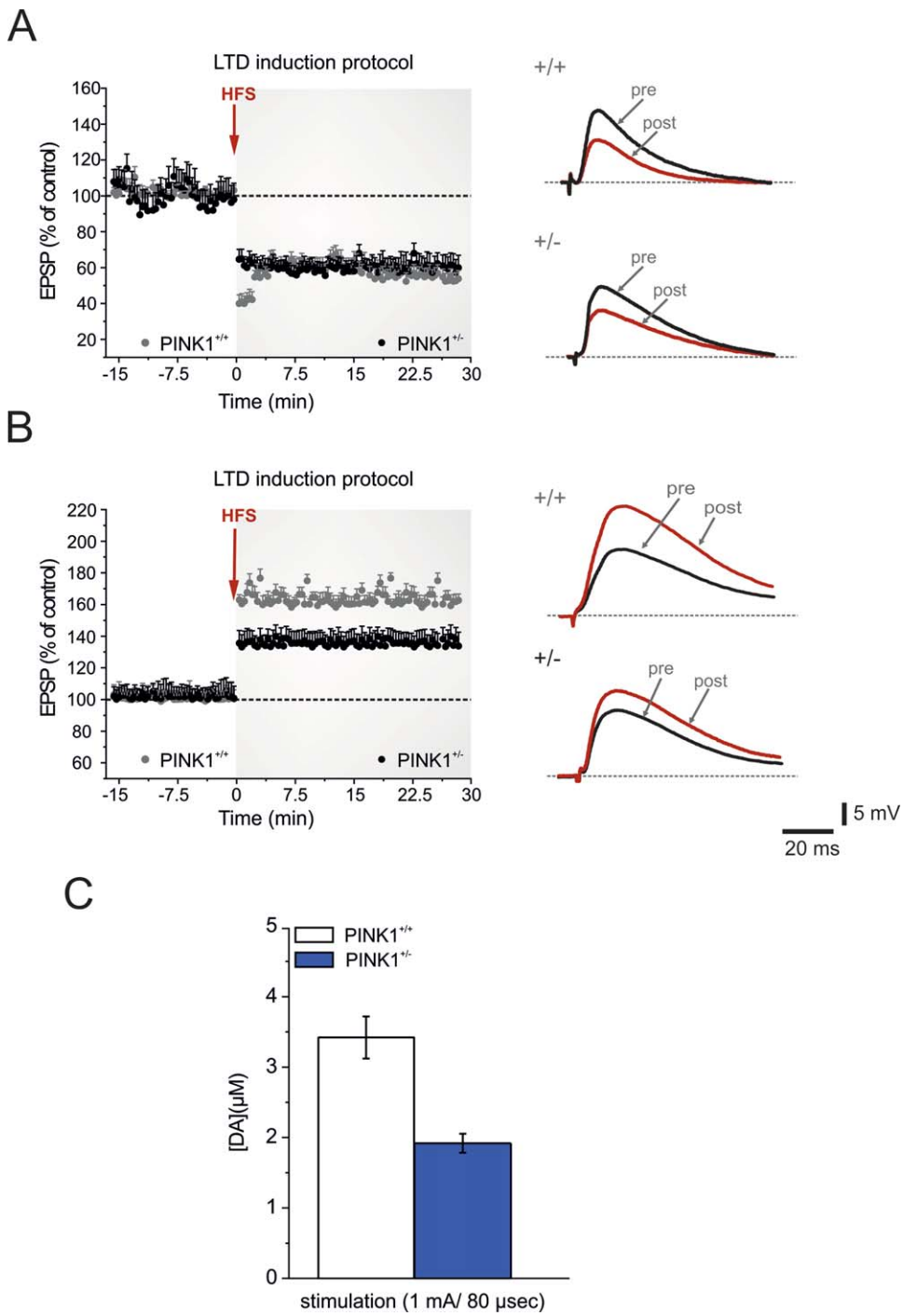

FIG. 4. Selective long-term potentiation (LTP) impairment in heterozygous phosphatase and tensin homolog-induced putative kinase 1 (*PINK1*) knockout (PINK1$^{+/-}$) mice is associated with reduced dopamine (DA) overflow. (**A**) The time course of long-term depression (LTD) in wild-type (PINK1$^{+/+}$) mice and PINK1$^{+/-}$ mice was recorded from parasagittal slices. High-frequency stimulation (HFS) (arrow) induces robust LTD in both genotypes. Superimposed traces of excitatory postsynaptic potentials (EPSPs) were recorded before (pre) and 20 minutes after (post) HFS in PINK1$^{+/+}$ and PINK1$^{+/-}$ medium spiny neurons (MSNs). (**B**) The LTP induction protocol causes normal LTP in PINK1$^{+/+}$ MSNs (gray circles), whereas the magnitude of LTP recorded in PINK1$^{+/-}$ mice is significantly lower (black circles). Sample traces of EPSPs recorded before and after HFS indicate that synaptic potentiation is of significantly lower magnitude in PINK1$^{+/-}$ MSNs. (**C**) Amperometric measurement of striatal extracellular DA levels ([DA]; expressed in μM) in PINK1$^{+/-}$ mice is compared with the levels in PINK1$^{+/+}$ mice. The graph illustrates striatal extracellular DA levels in response to supramaximal stimulation (1 mA, 80 μsec). In PINK1$^{+/-}$ mice, striatal DA release is significant lower than in PINK1$^{+/+}$ mice. Each value is expressed as the mean ± standard error of the mean. [Color figure can be viewed in the online issue, which is available at wileyonlinelibrary.com.]

To support the hypothesis that an impairment of DA release could play a major role in the LTP deficit, we performed amperometric recordings in striatal slices. Indeed, in response to electrical stimulation, the striatal extracellular DA release evoked in PINK1$^{+/-}$ slices was significantly lower

compared with that evoked in PINK1$^{+/+}$ slices (Fig. 4C).

Increasing Dopamine Release Restores Corticostriatal Long-term Potentiation

It is well established that D1Rs play a crucial role in the control of striatal LTP.[38,39] Thus, we pretreated striatal slices with the selective D1R agonist SKF38393 (10 μM, 20 minutes), which failed to restore LTP (141% ± 4.2%; $n = 9$; $P < 0.05$; Mann-Whitney test) (Fig. 5A). In an attempt to increase the available amount of DA for release upon stimulation, we pretreated striatal slices with the DA precursor L-dopa (100 μM, 30–45 minutes before the LTP-induction protocol). In this condition, we recorded a partial LTP rescue in PINK1$^{+/-}$ MSNs (151.7% ± 7.3%; n = 8; $P < 0.05$; t test) (Fig. 5A).

Next, to distinguish between a potential failure of the reuptake process and a deficient DA release, slices were pretreated with nomifensine (100 μM, 30 minutes), a DA-reuptake inhibitor, or with the DA releaser amphetamine (100 μM, 30 minutes). Nomifensine was ineffective in rescuing LTP in PINK1$^{+/-}$ MSNs (135.5% ± 8.3%, n = 6; $P > 0.05$; t test) (Fig. 5B). Conversely, amphetamine induced a complete recovery of striatal LTP in PINK1$^{+/-}$ MSNs (172.3% ± 7.9%; n = 11; $P < 0.05$; Mann-Whitney test) (Fig. 5B) to levels comparable to the levels measured in PINK1$^{+/+}$ MSNs.

The finding that amphetamine could restore LTP led us to test a number of pharmacological agents capable of increasing synaptic DA levels. In a first set of experiments, we tested the *trace amine* tyramine, the action of which relies on the ability to release catecholamines in an amphetamine-like manner through the displacement from synaptic vesicles, promoting the reversal of plasma membrane transporters.[40] Pretreatment of striatal slices with tyramine (10 μM, 30-45 minutes) was followed by a complete rescue of striatal

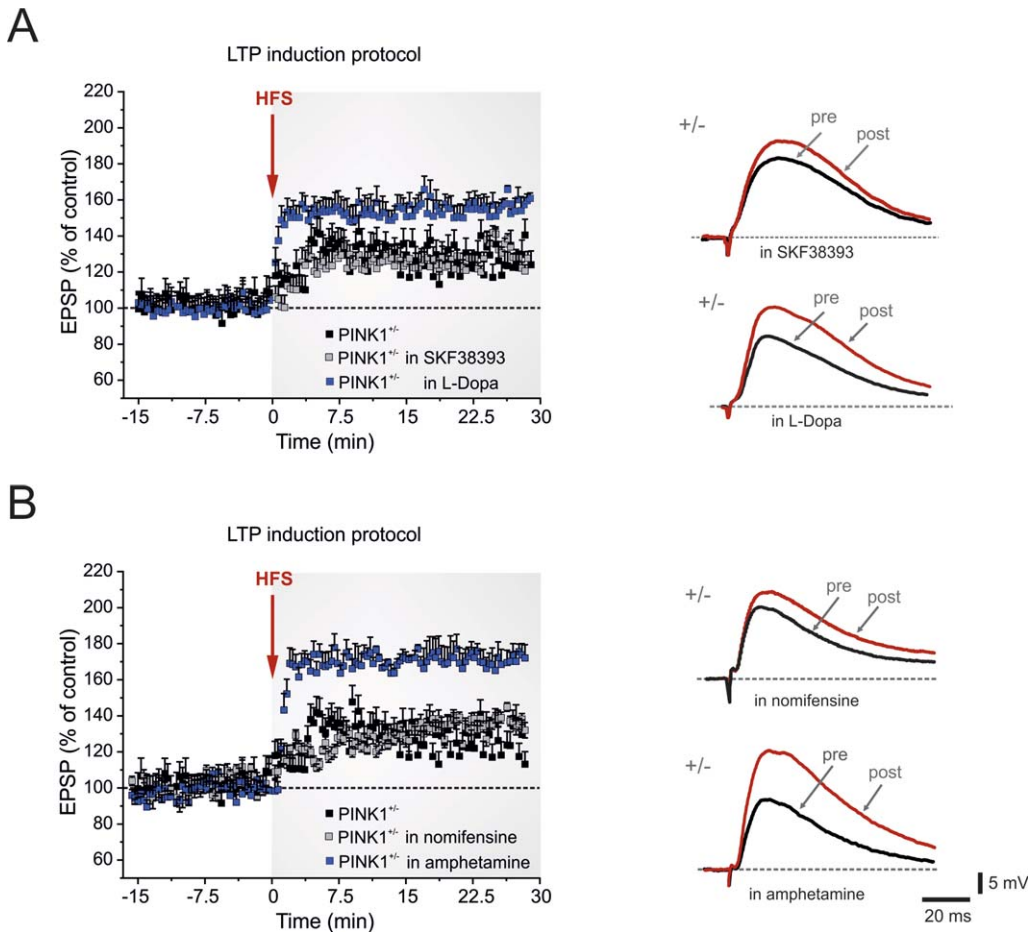

FIG. 5. Dopamine (DA) dependence of long-term potentiation (LTP) deficit is illustrated in heterozygous phosphatase and tensin homolog-induced putative kinase 1 (*PINK1*) knockout (PINK1$^{+/-}$) mice. (**A**) Pretreatment of slices with the D1R receptor agonist SKF38393 (10 μM, 20 minutes) does not restore LTP (gray squares). Conversely, a partial rescue is observed after slice preincubation with levodopa (L-dopa) (100 μM, 30–45 minutes; blue squares). (**B**) Preincubation (pre) with 10 μM nomifensine (30 minutes), a DA-reuptake inhibitor, is unable to rescue LTP (gray squares), whereas amphetamine (100 μM, 30 minutes) restores LTP in PINK1$^{+/-}$ medium spiny neurons to control levels (blue squares). Superimposed excitatory post-synaptic potentials (EPSPs) illustrate the recovery of LTP by amphetamine pretreatment (post) compared with the lack of effect by nomifensine. Each data point represents the mean ± standard error of the mean from > 12 independent observations. HFS indicates high-frequency stimulation. [Color figure can be viewed in the online issue, which is available at wileyonlinelibrary.com.]

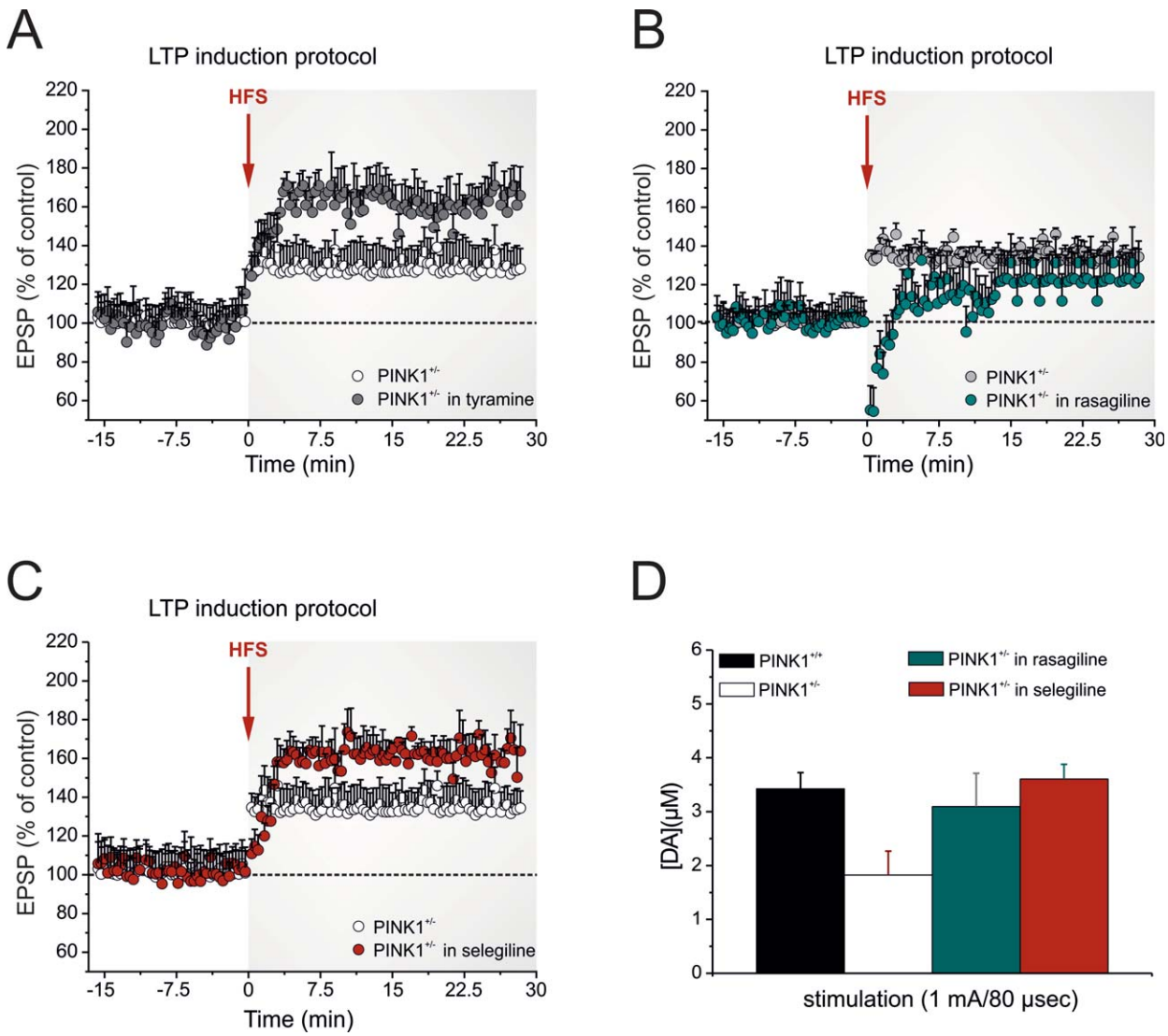

FIG. 6. Increasing dopamine (DA) availability restores both long-term potentiation (LTP) deficits and striatal DA content. (**A**) Preincubation of slices with the trace amine tyramine (10 μM, 30–45 minutes) is able to restore the LTP deficit recorded in heterozygous phosphatase and tensin homolog-induced putative kinase 1 (*PINK1*) knockout mice (PINK1$^{+/-}$). (**B**) Rasagiline (10 μM, 30–45 minutes) fails to rescue LTP, whereas (**C**) selegiline (30 μM, 2-hour slice preincubation) restores LTP in PINK1$^{+/-}$ medium spiny neurons. Each data point represents the mean ± standard error of the mean from > 12 independent observations. EPSP indicates excitatory postsynaptic potentials; HFS, high-frequency stimulation. (**D**) Measurements of striatal extracellular DA concentrations ([DA]; expressed in μM) in PINK1$^{+/-}$ mice indicate that both selegiline and rasagiline are able to restore physiologic DA levels in response to supramaximal stimulation. Each value is expressed as the mean ± standard error of the mean. [Color figure can be viewed in the online issue, which is available at wileyonlinelibrary.com.]

LTP in PINK1$^{+/-}$ MSNs (163% ± 11.8%; $n = 8$; $P < 0.01$; t test) (Fig. 6A).

The selective inhibition of brain monoamine oxidase B (MAO-B) results in extension of the availability and activity of endogenous DA in the striatum through blockade of its degradation.[15,41] First, we tested rasagiline (10 μM, 30-45 minutes), which, per se, did not cause a significant change in EPSP amplitude but failed to rescue LTP (121.6% ± 11.3%; $n = 9$; $P > 0.05$; Mann-Whitney test) (Fig. 6B). Selegiline, along with blocking MAO-B in an irreversible manner, also acts on neurotransmitter vesicular release through its amphetamine-like metabolite.[42,43] Indeed, slice preincubation with selegiline (30 μM, 2 hours before HFS) resulted in the full rescue of striatal LTP (164.7% ± 10.1%; $n = 11$; $P < 0.01$ Mann-Whitney test) (Fig. 6C). Our electrophysiological findings were paralleled by a set of amperometric recordings, which showed that pretreatment with selegiline (30 μM; n = 18; $P < 0.05$) completely rescued striatal DA content, whereas application of rasagiline (10 μM; n = 14; $P < 0.05$) only partially restored evoked DA release (Fig. 6D).

Discussion

Compelling evidence obtained from animal models of monogenic forms of PD has demonstrated

remarkable abnormalities of DA-mediated neurotransmission and corticostriatal synaptic plasticity indicative of a fundamental distortion of network function within the basal ganglia[14,16] (for reviews, see Madeo et al.[44] and Klein et al.[45]). Recent neuroimaging studies of non-manifesting carriers of heterozygous mutations in the *Parkin* or *PINK1* genes have unequivocally shown that a single mutant allele is associated with a dopaminergic nigrostriatal dysfunction that conveys an increased risk of developing PD throughout an individual's lifetime.[46-49]

Our findings provide novel evidence for a plausible cellular and synaptic correlate of the subclinical motor impairment observed in non-manifesting *PINK1* heterozygotes and have relevant pathophysiological implications for the role of *PINK1* heterozygous mutations on DA-dependent synaptic plasticity. Along with our behavioral analyses, we demonstrated that, in heterozygous knockout mice, morphology and basic physiological cellular activity of both nigral and striatal neurons are preserved. However, a significant decrease in evoked DA release paralleled a subtle alteration of LTP, whereas LTD expression was normal. More important, we report that drugs capable of promoting DA release in an amphetamine-like manner are able to restore plasticity deficits.

This study represents the first evidence that *PINK1* haploinsufficiency differentially affects the expression of two distinct forms of corticostriatal synaptic plasticity. In fact, our data show a normal LTD and selective alteration of LTP in heterozygous PINK1 mice; whereas, in homozygous PINK1 mice, both forms of corticostriatal synaptic plasticity were impaired.[14] The precise process leading to such specific deficit of synaptic plasticity in the heterozygous condition remains to be established. We can hypothesize that the two distinct forms of synaptic plasticity may reflect different stages of the disease course. In heterozygotes, when only one wild-type PINK1 allele is normally functioning, the LTD is normally expressed; whereas the disruption of both PINK1 alleles, as observed in the presence of homozygous or compound heterozygous mutations, represents a condition that is both necessary and sufficient to determine the complete disruption of bidirectional corticostriatal synaptic plasticity. In support of this hypothesis, recent data emerging from a study conducted on a rodent model of early PD suggest that distinct degrees of DA denervation differentially affect the induction and maintenance of both corticostriatal LTP and LTD.[50] It is well accepted that the maintenance of dopaminergic tone governing striatal output is essential to preserve motor control.[51,52] Hence, the presence of a single mutant PINK1 allele may reflect an initial breakdown of striatal DA homeostasis, which, in turn, influences the normal expression of striatal synaptic plasticity. These findings support the hypothesis that nigrostriatal dopaminergic dysfunction gives rise to an early dysfunction of basal ganglia circuits during the presymptomatic phase of the disease, which appears to be in agreement with our evidence of a normal motor behavior. A latent dopaminergic nigrostriatal dysfunction also has been found in non-manifesting individuals who carry heterozygous mutations in other autosomal recessive PD genes, such as *Parkin*.[53-55] Functional studies have demonstrated that a compensatory mechanism characterized by the recruitment of cortical motor areas may counteract the preclinical nigrostriatal dysfunction to ensure a normal level of performance during a motor sequence task.[9,10,53,54]

At the cellular level, available experimental evidence suggests that the complete expression of LTP requires a large amount of energy to enable the mobilization of synaptic vesicles from the reserve pool, which is recruited only after HFS.[56,57] *PINK1* plays an important role in cellular energy maintenance under increased demand, and *PINK1* deficiency is related to mitochondrial respiratory defects.[58,59] Indeed, several reports have indicated that mitochondria are essential for synaptic vesicle release under conditions of intense neuronal activity through vesicle mobilization from the reserve pool, a process that requires numerous ATP-consuming steps.[60-62] Accordingly, it is plausible that a mitochondrial dysfunction may distinctively impact the maintenance of sufficient cellular ATP, affecting the synaptic vesicle cycling required for synaptic plasticity induction. Studies from *Drosophila* reveal that deficiency or inactivation of *PINK1* is associated with an impairment of mobilization of the reserve pool during intense stimulation, affecting synaptic function.[59] More recently, studies from rodent models focused on the role of PINK1 in mitochondrial respiration have suggested that loss of PINK1 causes defects in mitochondrial transmembrane potential through dysregulation of the mitochondrial permeability transition pore opening.[58] Thus, it is conceivable that changes in the mitochondrial ability to regenerate ATP may affect the magnitude of synaptic vesicle release at presynaptic terminals, primarily through ATP synthesis.

A clear finding that emerges from our work is the DA-dependence of striatal plasticity, which has been a matter of intense investigation.[63,64] Indeed, our data indicate a significant decrement in synaptic DA release at high frequencies of stimulation. Accordingly, displacement of neurotransmitter from storage areas to the synaptic cleft is able to restore LTP deficit, as observed with amphetamine, a DA releaser, but not with nomifensine, an uptake blocker. Notably, drugs that exhibited a similar, amphetamine-like pharmacodynamic profile, such as tyramine and selegiline, restored LTP. Trace amines are found at low

concentrations in neuronal tissues, where they are packed and released along with traditional amine compounds.[65] It has been demonstrated that trace amines displace active biogenic amines and act on transporters in an amphetamine-like manner, thereby promoting DA release and new DA synthesis.[66,67]

Currently, strategies for treating PD consider MAO-B inhibitors, because they increase DA levels by blocking its degradation.[15,41,68,69] Indeed, DA levels are finely tuned by MAO enzymes, which exist in two functional isoforms: MAO-A and MAO-B. In line with current literature, our amperometric measurements revealed that, although to a different extent, both rasagiline and selegiline are able to increase DA striatal levels in PINK1$^{+/-}$ mice compared with controls. However, we observed that only selegiline treatment was able to restore normal LTP expression. This is not surprising, because the pharmacological properties of these two MAO-B inhibitors may account for such differences. In fact, selegiline and rasagiline exhibit distinct pharmacokinetic properties. Selegiline is metabolized in vivo to 1-amphetamine and to 1-methamphetamine[68] and has amphetamine-like properties[69]; whereas rasagiline is metabolized to aminoindan, which is devoid of amphetamine-like actions.[70] Therefore, it is conceivable that the LTP rescue in PINK1 heterozygous mice is determined by the ability to force release from synaptic vesicles. The abnormalities of synaptic plasticity described in heterozygous mice might be considered an endophenotype to this monogenic form of PD and a valid tool with which to design potentially disease-modifying therapies. This appears to be an intriguing working hypothesis, although results obtained from mouse models need to be interpreted with caution and further refined with additional analyses. ■

Acknowledgements: We thank Mr. M. Tolu and V. Batocchi for their excellent technical assistance.

References

1. Puschmann A. Monogenic Parkinson's disease and parkinsonism: clinical phenotypes and frequencies of known mutations. Parkinsonism Rel Dis 2013;19:407-415.
2. Samaranch L, Lorenzo-Betancor O, Arbelo JM, et al. PINK1-linked parkinsonism is associated with Lewy body pathology. Brain 2010;133:1128-1142.
3. Marongiu R, Ferraris A, Ialongo T, et al. PINK1 heterozygous rare variants: prevalence, significance and phenotypic spectrum [serial online]. Hum Mutat 2008;29:565.
4. Ibanez P, Lesage S, Lohmann E, et al. Mutational analysis of the PINK1 gene in early-onset parkinsonism in Europe and North Africa. Brain 2006;129:686-694.
5. Dauer W, Przedborski S. Parkinson's disease: mechanisms and models. Neuron 2003;39:889-909.
6. Calabresi P, Di Filippo M, Gallina A, et al. New synaptic and molecular targets for neuroprotection in Parkinson's disease. Mov Disord 2013;28:51-60.
7. Morrish PK, Sawle GV, Brooks DJ. Regional changes in [18F]dopa metabolism in the striatum in Parkinson's disease. Brain 1996; 119(pt 6):2097-2103.
8. Hilker R, Schweitzer K, Coburger S, et al. Nonlinear progression of Parkinson disease as determined by serial positron emission tomographic imaging of striatal fluorodopa F 18 activity. Arch Neurol 2005;62:378-382.
9. van Nuenen BF, Weiss MM, Bloem BR, et al. Heterozygous carriers of a Parkin or PINK1 mutation share a common functional endophenotype. Neurology 2009;72:1041-1047.
10. van Nuenen BF, van Eimeren T, van der Vegt JP, et al. Mapping preclinical compensation in Parkinson's disease: an imaging genomics approach. Mov Disord 2009;24(suppl 2):S703-S710.
11. Eggers C, Schmidt A, Hagenah J, et al. Progression of subtle motor signs in PINK1 mutation carriers with mild dopaminergic deficit. Neurology 2010;74:1798-1805.
12. Khan NL, Valente EM, Bentivoglio AR, et al. Clinical and subclinical dopaminergic dysfunction in PARK6-linked parkinsonism: an 18F-dopa PET study. Ann Neurol 2002;52:849-853.
13. Fiorio M, Valente EM, Gambarin M, et al. Subclinical sensory abnormalities in unaffected PINK1 heterozygotes. J Neurol 2008; 255:1372-1377.
14. Kitada T, Pisani A, Porter DR, et al. Impaired dopamine release and synaptic plasticity in the striatum of PINK1-deficient mice. Proc Natl Acad Sci U S A 2007;104:11441-11446.
15. Mercuri NB, Scarponi M, Bonci A, Siniscalchi A, Bernardi G. Monoamine oxidase inhibition causes a long-term prolongation of the dopamine-induced responses in rat midbrain dopaminergic cells. J Neurosci 1997;17:2267-2272.
16. Goldberg MS, Pisani A, Haburcak M, et al. Nigrostriatal dopaminergic deficits and hypokinesia caused by inactivation of the familial Parkinsonism-linked gene DJ-1. Neuron 2005;45:489-496.
17. Martella G, Tassone A, Sciamanna G, et al. Impairment of bidirectional synaptic plasticity in the striatum of a mouse model of DYT1 dystonia: role of endogenous acetylcholine. Brain 2009; 132(pt 9):2336-2349.
18. Ding J, Peterson JD, Surmeier DJ. Corticostriatal and thalamostriatal synapses have distinctive properties. J Neurosci 2008;28:6483-6492.
19. Cossart R, Hirsch JC, Cannon RC, et al. Distribution of spontaneous currents along the somato-dendritic axis of rat hippocampal CA1 pyramidal neurons. Neuroscience 2000;99:593-603.
20. Cuomo D, Martella G, Barabino E, et al. Metabotropic glutamate receptor subtype 4 selectively modulates both glutamate and GABA transmission in the striatum: implications for Parkinson's disease treatment. J Neurochem 2009;109:1096-1105.
21. Mercuri NB, Stratta F, Calabresi P, Bonci A, Bernardi G. Activation of metabotropic glutamate receptors induces an inward current in rat dopamine mesencephalic neurons. Neuroscience 1993; 56:399-407.
22. Mercuri NB, Bonci A, Johnson SW, Stratta F, Calabresi P, Bernardi G. Effects of anoxia on rat midbrain dopamine neurons. J Neurophysiol 1994;71:1165-1173.
23. Napolitano F, Bonito-Oliva A, Federici M, et al. Role of aberrant striatal dopamine D1 receptor/cAMP/protein kinase A/DARPP32 signaling in the paradoxical calming effect of amphetamine. J Neurosci 2010;30:11043-11056.
24. Mercuri NB, Bonci A, Calabresi P, Stefani A, Bernardi G. Properties of the hyperpolarization-activated cation current Ih in rat midbrain dopaminergic neurons. Eur J Neurosci 1995;7:462-469.
25. Kawagoe KT, Wightman RM. Characterization of amperometry for in vivo measurement of dopamine dynamics in the rat brain. Talanta 1994;41:865-874.
26. Schmitz Y, Lee CJ, Schmauss C, Gonon F, Sulzer D. Amphetamine distorts stimulation-dependent dopamine overflow: effects on D2 auto-receptors, transporters, and synaptic vesicle stores. J Neurosci 2001;21:5916-5924.
27. Sciamanna G, Tassone A, Mandolesi G, et al. Cholinergic dysfunction alters synaptic integration between thalamostriatal and corticostriatal inputs in DYT1 dystonia. J Neurosci 2012;32: 11991-12004.
28. Ventura R, Alcaro A, Cabib S, Conversi D, Mandolesi L, Puglisi-Allegra S. Dopamine in the medial prefrontal cortex controls genotype-dependent effects of amphetamine on mesoaccumbens dopamine release and locomotion. Neuropsychopharmacology 2004;29:72-80.

29. Spink AJ, Tegelenbosch RA, Buma MO, Noldus LP. The EthoVision video tracking system—a tool for behavioral phenotyping of transgenic mice. Physiol Behav 2001;73:731-744.
30. Glasl L, Kloos K, Giesert F, et al. Pink1-deficiency in mice impairs gait, olfaction and serotonergic innervation of the olfactory bulb. Exp Neurol 2012;235:214-227.
31. Grinberg LT, Rueb U, Alho AT, Heinsen H. Brainstem pathology and non-motor symptoms in PD. J Neurol Sci 2010;289 (1-2):81-88.
32. Jellinger KA. Synuclein deposition and non-motor symptoms in Parkinson disease. J Neurol Sci 2011;310(1-2):107-111.
33. Smith GA, Isacson O, Dunnett SB. The search for genetic mouse models of prodromal Parkinson's disease. Exp Neurol 2012;237: 267-273.
34. Lacey MG, Mercuri NB, North RA. Dopamine acts on D2 receptors to increase potassium conductance in neurones of the rat substantia nigra zona compacta. J Physiol 1987;392:397-416.
35. Kitada T, Pisani A, Karouani M, et al. Impaired dopamine release and synaptic plasticity in the striatum of Parkin −/− mice. J Neurochem 2009;110:613-621.
36. Tozzi A, de Iure A, Di Filippo M, et al. the distinct role of medium spiny neurons and cholinergic interneurons in the D2/A2A receptor interaction in the striatum: implications for Parkinson's disease. J Neurosci 2011;31:1850-1862.
37. Calabresi P, Pisani A, Mercuri NB, Bernardi G. Long-term potentiation in the striatum is unmasked by removing the voltage-dependent magnesium block of NMDA receptor channels. Eur J Neurosci 1992;4:929-935.
38. Centonze D, Gubellini P, Picconi B, et al. An abnormal striatal synaptic plasticity may account for the selective neuronal vulnerability in Huntington's disease. Neurol Sci 2001;22:61-62.
39. Kerr JN, Wickens JR. Dopamine D-1/D-5 receptor activation is required for long-term potentiation in the rat neostriatum in vitro. J Neurophysiol 2001;85:117-124.
40. Ledonne A, Berretta N, Davoli A, Rizzo GR, Bernardi G, Mercuri NB. Electrophysiological effects of trace amines on mesencephalic dopaminergic neurons [serial online]. Front Syst Neurosci 2011;5: 56.
41. Dimpfel W, Hoffmann JA. Electropharmacograms of rasagiline, its metabolite aminoindan and selegiline in the freely moving rat. Neuropsychobiology 2010;62:213-220.
42. Schapira AHV. Monoamine oxidase B inhibitors for the treatment of Parkinson's disease. CNS Drugs 2011;25:1061-1071.
43. Engberg G, Elebring T, Nissbrandt H. Deprenyl (selegiline), a selective MAO-B inhibitor with active metabolites; effects on locomotor activity, dopaminergic neurotransmission and firing rate of nigral dopamine neurons. J Pharmacol Exp Ther 1991;259:841-847.
44. Madeo G, Martella G, Schirinzi T, Ponterio G, Shen J, Bonsi P, Pisani A. Aberrant striatal synaptic plasticity in monogenic parkinsonisms. Neuroscience 2012;211:126-135.
45. Picconi B, Piccoli G, Calabresi P. Synaptic dysfunction in Parkinson's disease. Adv Exp Med Biol 2012;970:553-572.
46. Klein C, Lohmann-Hedrich K, Rogaeva E, Schlossmacher MG, Lang AE. Deciphering the role of heterozygous mutations in genes associated with parkinsonism. Lancet Neurol 2007;6:652-662.
47. Hilker R, Klein C, Ghaemi M, et al. Positron emission tomographic analysis of the nigrostriatal dopaminergic system in familial parkinsonism associated with mutations in the parkin gene. Ann Neurol 2001;49:367-376.
48. Khan NL, Scherfler C, Graham E, et al. Dopaminergic dysfunction in unrelated, asymptomatic carriers of a single parkin mutation. Neurology 2005;64:134-136.
49. Walter U, Klein C, Hilker R, Benecke R, Pramstaller PP, Dressler D. Brain parenchyma sonography detects preclinical parkinsonism. Mov Disord 2004;1912:1445-1449.
50. Paille V, Picconi B, Bagetta V, et al. Distinct levels of dopamine denervation differentially alter striatal synaptic plasticity and NMDA receptor subunit composition. J Neurosci 2010;30:14182-14193.
51. Agid Y. Parkinson's disease: pathophysiology. Lancet 1991;337: 1321-1324.
52. Bezard E, Dovero S, Prunier C, et al. Relationship between the appearance of symptoms and the level of nigrostriatal degeneration in a progressive 1-methyl-4-phenyl-1,2,3,6-tetrahydropyridine-lesioned macaque model of Parkinson's disease. J. Neurosci 2001; 21:6853-6861.
53. Buhmann C, Binkofski F, Klein C, et al. Motor reorganization in asymptomatic carriers of a single mutant Parkin allele: a human model for presymptomatic parkinsonism. Brain 2005;128:2281-2290.
54. Schneider SA, Talelli P, Cheeran BJ, et al. Motor cortical physiology in patients and asymptomatic carriers of parkin gene mutations. Mov Disord 2008;23:1812-1819.
55. Khan NL, Brooks DJ, Pavese N, et al. Progression of nigrostriatal dysfunction in a Parkin kindred: an [18F]dopa PET and clinical study. Brain 2002;125:2248-2256.
56. Kuromi H, Kidokoro Y. Exocytosis and endocytosis of synaptic vesicles and functional roles of vesicle pools: lessons from the Drosophila neuromuscular junction. Neuroscientist 2005;11:138-147.
57. Rizzoli SO, Betz WJ. Synaptic vesicle pools. Nat Rev Neurosci 2005;6:57-69.
58. Gautier CA, Kitada T, Shen J. Loss of PINK1 causes mitochondrial functional defects and increased sensitivity to oxidative stress. Proc Natl Acad Sci U S A 2008;105:11364-11369.
59. Morais VA, Verstreken P, Roethig A, et al. Parkinson's disease mutations in PINK1 result in decreased complex I activity and deficient synaptic function. EMBO Mol Med 2090;1:99-111.
60. Vos M, Lauwers E, Verstreken P. Synaptic mitochondria in synaptic transmission and organization of vesicle pools in health and disease [serial online]. Front Synaptic Neurosci 2010;2:139.
61. Mochida S. Activity-dependent regulation of synaptic vesicle exocytosis and presynaptic short-term plasticity. Neurosci Res 2011; 70:16-23.
62. Ivannikov MV, Sugimori M, Llinas RR. Synaptic vesicle exocytosis in hippocampal synaptosomes correlates directly with total mitochondrial volume. J Mol Neurosci 2013;49:223-230.
63. Calabresi P, Picconi B, Tozzi A, Di Filippo M. Dopamine-mediated regulation of corticostriatal synaptic plasticity. Trends Neurosci 2007;30:211-219.
64. Nicola SM, Surmeier J, Malenka RC. Dopaminergic modulation of neuronal excitability in the striatum and nucleus accumbens. Annu Rev Neurosci 2000;23:185-215.
65. Parker EM, Cubeddu LX. Comparative effects of amphetamine, phenylethylamine and related drugs on dopamine efflux, dopamine uptake and mazindol binding. J Pharmacol Exp Ther 1988;245: 199-210.
66. Bailey BA, Philips SR, Boulton AA. In vivo release of endogenous dopamine, 5-hydroxytryptamine and some of their metabolites from rat caudate nucleus by phenylethylamine. Neurochem Res 1987;12:173-178.
67. Geracitano R, Federici M, Prisco S, Bernardi G, Mercuri NB. Inhibitory effects of trace amines on rat midbrain dopaminergic neurons. Neuropharmacology 2004;46:807-814.
68. Reynolds GP, Elsworth JD, Blau K, Sandler M, Lees AJ, Stern GM. Deprenyl is metabolized to methamphetamine and amphetamine in man. Br J Clin. Pharmacol 1978;6:542-544.
69. Simpson LL. Evidence that deprenyl, a type B monoamine oxidase inhibitor, is an indirectly acting sympathomimetic amine. Biochem Pharmacol 1978;27:1591-1595.
70. Youdim MB, Gross A, Finberg JP. Rasagiline [N-propargyl-1R(fl)-aminoindan], a selective and potent inhibitor of mitochondrial monoamine oxidase B. Br J Pharmacol 2001;132:500-506.